

THE OFFICIAL MAGAZINE OF THE OCEANOGRAPHY SOCIETY

Oceanography

CITATION

Cazau, D., C. Pradalier, J. Bonnel, and C. Guinet. 2017. Do southern elephant seals behave like weather buoys? *Oceanography* 30(2):140–149, <https://doi.org/10.5670/oceanog.2017.236>.

DOI

<https://doi.org/10.5670/oceanog.2017.236>

COPYRIGHT

This article has been published in *Oceanography*, Volume 30, Number 2, a quarterly journal of The Oceanography Society. Copyright 2017 by The Oceanography Society. All rights reserved.

USAGE

Permission is granted to copy this article for use in teaching and research. Republication, systematic reproduction, or collective redistribution of any portion of this article by photocopy machine, reposting, or other means is permitted only with the approval of The Oceanography Society. Send all correspondence to: info@tos.org or The Oceanography Society, PO Box 1931, Rockville, MD 20849-1931, USA.



Do Southern Elephant Seals Behave Like Weather Buoys?

By Dorian Cazau, Cédric Pradalier, Julien Bonnel, and Christophe Guinet

ABSTRACT. Biologging using Kerguelen Islands' southern elephant seals (SES; *Mirounga leonina*) has been widely used to collect environmental parameters of the Southern Ocean. This study evaluates whether raw accelerometer and magnetometer data from biologging of SES can be used to predict above-surface wind conditions and wave period and height. From these sensors, SES behavior during post-dive surfacing time has been modeled with the Euler angles pitch, roll, and yaw. Environmental variables (i.e., wind orientation, wind speed, significant wave height, and mean wave period) have been extracted from the European Centre for Medium-Range Weather Forecasts (ECMWF) database, which assimilates satellite images into models to provide high-resolution environmental data. SES behavioral and environmental variables are analyzed together to test two hypotheses: (1) SES behavior is constrained by wind speed and/or direction, and (2) SES can be used as weather buoys to estimate wave parameters. Significant pair-wise correlation relations were observed, for example, between SES heading (i.e., yaw) and wind direction. SES vertical displacement was sufficient to estimate the mean wave period with a root-mean-square error below 2 s. Overall, biologged SES tend to orient their heads with the prevailing wind behind them, and are good ocean surface followers, showing great promise for the use of biologged SES as a proxy to collect reliable information on wind and wave conditions. Conversely, this study also suggests that SES respond to environmental conditions to optimize their energy recovery during post-dive surfacing time.

INTRODUCTION

The use of animal-borne autonomous recording tags (i.e., biologging) is becoming widespread (Ropert-Coudert and Wilson, 2005; Rutz and Hays, 2009), and allows the acquisition of large environmental data sets (e.g., temperature, salinity, light, fluorescence). Such biologged animals move freely in their natural environment, sampling the water column at high resolution over large temporal and spatial scales. Among top marine predators, air-breathing diving species such as southern elephant seals (SES) (*Mirounga leonina*) of the Kerguelen Islands (49.54°S, 70.21°E) are appealing animals to use for biologging because of

their broad migrations and large size that allows them to carry electronic devices with minimal disturbance. Post-breeding adult females from Kerguelen forage mainly in oceanic waters of the Antarctic and polar frontal zones (below 60°S) from October to January (Bailleul et al., 2010). The biologging devices are glued to SES while they are on land in their breeding colonies. Their closed-loop migratory routes also provide the opportunity to use Acoustimetrics Acousondes™ (miniature, self-contained, autonomous acoustic recorders designed for underwater use) that can be retrieved at the end of the migration.

While strong east-west current speeds

and the presence of sea ice off the Antarctic continent make the use of regular oceanographic instruments challenging, these harsh environmental conditions are not a problem for SES. Similar to underwater gliders, SES follow an up-and-down, sawtooth-like profile through the water column. SES dive to mesopelagic depths (300–500 m, up to 2,000 m), and spend up to 90% of their time at sea diving, with dives lasting on average between 20 and 30 minutes, resulting in surface intervals of approximately two to three minutes (Hindell, 1991).

SES are efficient, cost-effective, autonomous samplers of Southern Ocean environmental parameters. They have been widely recruited to fill a “blind spot” in Southern Ocean sampling coverage, having collected 90% of the oceanographic data (mainly vertical profiles of temperature and salinity) available south of 60°S since 2004 (Charrassin et al., 2008; Guinet et al., 2013). Classical weather buoys, for example, those that send data to the US National Oceanic and Atmospheric Administration's National Data Buoy Center (<http://www.ndbc.noaa.gov>) are very scarce south of 40°S. Various research programs such as the Marine Mammals Exploring the Oceans Pole to Pole (MEOP) consortium (<http://meop.net>; see also Treasure et al., 2017, in this issue) and the French Mammifère marin Echantillonneur du Milieu Océanique (MEMO; in English, “Mammals as Samplers of the Ocean Environment”) observatory and SO-MEMO ensure the

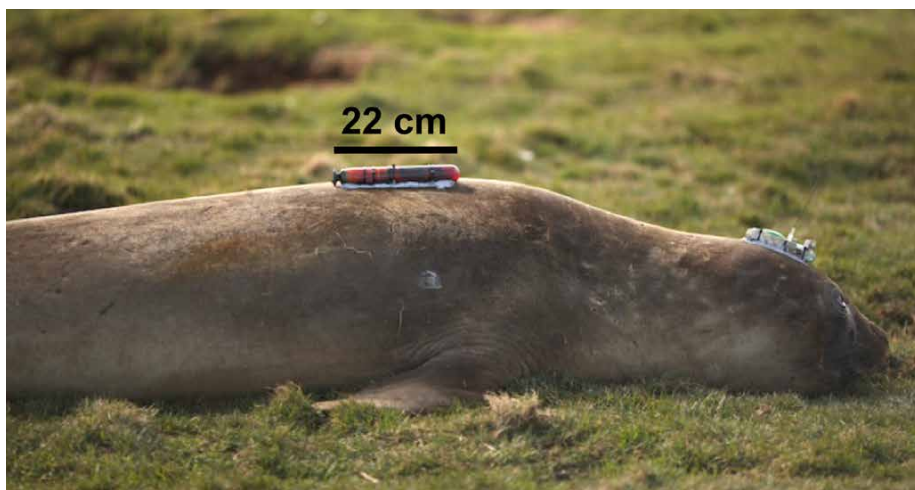


FIGURE 1. Photo of a biologged female southern elephant seal (SES). The red 22 cm instrument is the Acousonde™ 3A.

maintenance of this innovative and invaluable observation tool in the Southern Ocean. These research programs have already provided considerable biological information (e.g., on SES behavior and physiology and/or oceanographic information (e.g., physical and biogeochemical data on the marine environment).

On the biological side, Guinet et al. (2014) investigated SES foraging behavior, relating seal diving depth and prey encounter events to water temperature at 200 m depth as well as to light level at the surface and at depth. Richard et al. (2014) studied swimming effort and speed to monitor density variations of SES throughout their foraging excursions. More recently, acoustic data have been used to investigate behavioral and ecophysiological (breathing rate) parameters (Génin et al., 2015; Day et al., 2017).

On the oceanographic side, MEOP and MEMO/SO-MEMO are responsible for collection of considerable conductivity-temperature-depth (CTD) and time-depth recorder (TDR) data from the Southern Ocean. The quality-controlled MEOP-CTD and MEOP-TDR databases are publicly available to the scientific and operational oceanographic communities. Through such data collection, new

insights into water masses, oceanographic processes, and global ocean climate have been gained (Roquet et al., 2014). In particular, the seals have provided a marked increase in the number of hydrographic profiles from the sea ice zone, allowing mapping of major fronts south of 60°S and inference of sea ice formation rates from changes in upper-ocean salinity (Charrassin et al., 2008). Seals were also used to quantify phytoplankton concentration (Guinet et al., 2013) and to collect data for the first complete assessment of dense shelf water formation in Prydz Bay, which improved understanding of the production of globally important Antarctic Bottom Water (Williams et al., 2016). SES were also used as acoustic gliders of opportunity to estimate above-surface meteorological conditions from ocean ambient noise, with promising results obtained for wind speed estimation by Cazau et al. (2017), with an accuracy error of 2 m s⁻¹. The full list of papers using MEOP data, categorized into oceanography and biology, is available from: <http://meop.net/publications.html>.

This current study is intended to provide proof-of-concept for measurements of ocean environmental parameters that have not been explored in past

research on biologged SES, in particular, above-surface wind conditions and wave period and height. These parameters are routinely monitored by classical weather buoys that collect weather and ocean data across the world ocean (Gillhousen, 2007). These buoys can be either moored or free drifting, with sensor packages that generally each include a tilt-compensated triaxial accelerometer and magnetometer to measure wave parameters as well as a wind sensor (Daniault et al., 1985). The biologging tags on the SES also include a triaxial accelerometer and magnetometer.

The main objective of this current study is to explore whether ocean environmental parameters influence SES behavior during post-dive surfacing time, and whether the raw data can be converted into proxies to reliably estimate wind and wave parameters. The full three-dimensional dynamical behavior of SES at the ocean surface has been modeled with the well-known Euler angles pitch, roll, and yaw, as well as with the horizontally projected vertical acceleration, which can be double-integrated to extract vertical displacement. The ocean environmental parameters selected for this study are wind direction and speed (measured 10 m above sea surface), significant wave height, and mean wave period. They have been extracted from the European Centre for Medium-Range Weather Forecasts (ECMWF) database, and will be used here to ground truth these parameters.

MATERIAL AND METHODS

Material

During the austral springs of 2011 and 2012, four different post-breeding female SES with similar body characteristics were captured and equipped with data loggers on Kerguelen Island (Figure 1). These loggers included an Acousonde 3A device glued to the back of a seal on the longitudinal axis 10 cm behind the scapula; these devices have been used in previous

TABLE 1. Global information on the Acousonde data and time periods used for analysis.

Acousonde ID Number	Time Period (date)	Surface Interval Number/ Total Duration	Average Surface Phase Duration
A031	October 27, 2011–November 9, 2011	1541/61.9 h	2.1 min
A032	October 28, 2011–November 10, 2011	1632/64.3 h	3.6 min
626019	October 30, 2012–November 18, 2012	1359/65.7 h	2.8 min
626040	October 31, 2012–November 23, 2012	1746/75.6 h	3.9 min

research studies with marine mammals (e.g., Burgess et al., 1998, and Burgess, 2000). Care is taken to minimize the differences of tag alignment and positioning between one animal and the other. Besides passive acoustic data, which are not presented here, the Acousonde continuously recorded depth (via pressure), triaxial acceleration, and triaxial magnetometer data with a sampling frequency of 5 Hz. The three-axis compass onboard all Acousonde units is a Honeywell HMC1043. The Acousonde supports it with automatic hardware degaussing every time sampling starts. Table 1 provides details on the Acousondes and time periods used for analysis. Acousondes A031 and A032 were deployed during the austral spring of 2011 and were activated in the field at the same time so that their recording times overlapped. To save onboard storage space, a duty cycle was set up in each Acousonde that automatically turned it on for three hours of every 12-hour cycle. These two Acousondes recorded for approximately two weeks. Acousondes 626019 and 626040 were deployed in 2012 with the same setups, and recorded over three weeks using a duty cycle of four hours every 24 hours. Each SES was also equipped with a head-mounted Fast Loc GPS tag (Wildlife Computers) that provided GPS positions and ARGOS locations.

Our analysis uses only post-dive surface intervals. The R package Biologging tools developed by Yves le Bras of the Université de La Rochelle (available at <https://github.com/SESman/rbl>) are used to automatically detect the post-dive surface intervals of SES, based on pressure-derived depth and acceleration data. Ten

percent of the surface interval duration has been trimmed from the beginning and end of each phase to avoid any transient signals related to the SES raising their head above water or diving. Also, surface intervals shorter than 60 s were removed. All data processing and analyses were conducted using MATLAB. The record of total post-dive surface intervals was 37.4 hours long.

Figure 2 indicates the migratory routes followed by the SES during the time the Acousondes were active. The spatiotemporal coverage provided by these routes ranges from 71°E to 87°E and from 46°S to 52°S. SES provide local point measurements (like weather buoys) that are roughly uniformly distributed over these routes, with a sampling rate corresponding to their surfacing time (i.e., approximately every 25–30 minutes).

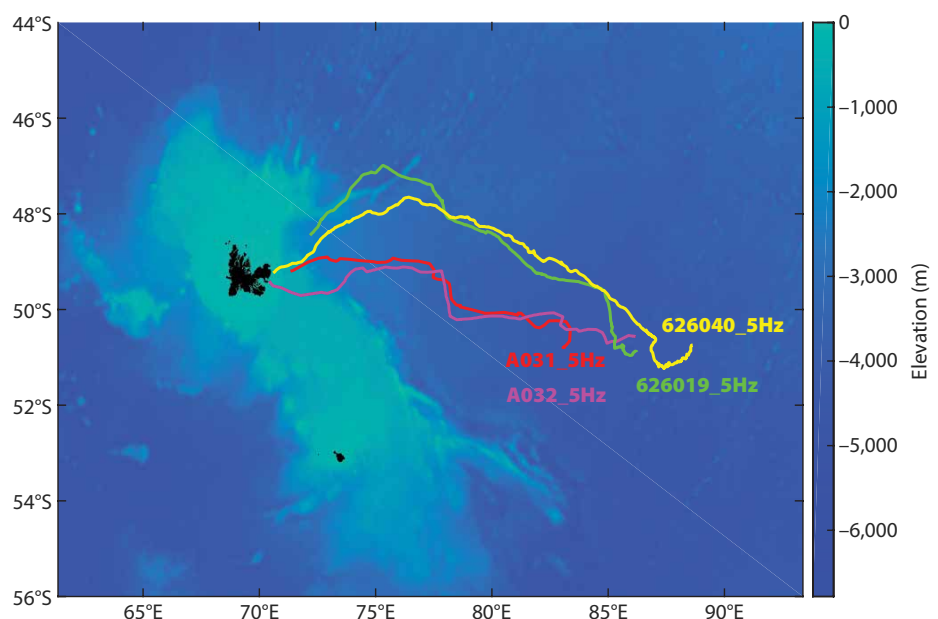


FIGURE 2. Migratory routes of the four different SES near the Kerguelen Islands (49.54°S, 70.21°E) in the Southern Ocean. See Table 1 for information on the Acousondes attached to the SES individuals.

ENVIRONMENTAL DATA

Environmental data were extracted from the ERA-Interim data set. Provided by ECMWF, ERA-Interim performs a reanalysis of the global atmosphere covering the data-rich period since 1979 (Dee et al., 2011). The atmospheric model is coupled to an ocean-wave model that resolves 30 wave frequencies and 24 wave directions at the nodes of its reduced $1.0^\circ \times 1.0^\circ$ latitude/longitude grid. Gridded data products include a large variety of three-hourly surface parameters that describe weather as well as ocean-wave and land-surface conditions, and six-hourly upper-air parameters that cover the troposphere and stratosphere. Berrisford et al. (2011) provide a detailed description of the ERA-Interim product archive.

Using a spatial resolution of 0.25° in longitude and latitude and a three-hour temporal resolution, we extracted the following variables from the ERA-Interim data set:

- u_{10} : The zonal wind component (m s^{-1}) 10 m above the sea surface
- v_{10} : The meridional wind component (m s^{-1}) 10 m above the sea surface
- swh : The significant wave height, defined as four times the square root

TABLE 2. List of all variables used for analysis and their ranges of values (as obtained after analyzing the corresponding data).

	Environment				Southern Elephant Seals' Behavior			
Variable	ψ_W	ϕ_W	swh	mwp	Pitch	Roll	Yaw	a_z^h
Definition	Wind Direction	Wind Speed	Significant Wave Height	Mean Wave Period	Rotation Around Lateral Axis	Rotation Around Longitudinal Axis	Rotation Around Normal Axis	Vertical Acceleration
Ranges and Unities	$[-2.8; 2.9]$ rad	$[2; 28]$ m s ⁻¹	$[1; 11]$ m	$[4; 17]$ s	$[-1.3; 1.4]$ rad	$[-1.1; 0.9]$ rad	$[-1.5; 1.5]$ rad	$[-3.2; 4.1]$ m s ⁻²

of the integral over all directions and all frequencies of the two-dimensional wave spectrum

- mwp: The spectral mean wave period(s), obtained using the reciprocal integral moment of the frequency wave spectrum, which is obtained by integrating the two-dimensional wave spectrum over all directions

Basic quality control of the data sets was performed to remove invalid data (e.g., wind speeds greater than 60 m s⁻¹). To allow comparison between wind components and the heading of the SES, we computed the angle $\psi_W = \text{atan2}(v10, u10)$ with *atan2* the arctangent function with two arguments¹, and the root-mean-square (RMS) norm of the wind speed vector $\phi_W = \sqrt{(u10^2 + v10^2)}$. Table 2 lists these environmental variables, as well as their ranges of values. Stopa and Cheung (2014) observed a consistent level of accuracy between the ECMWF reanalysis interim and reference values from Bullwinkle platforms, with RMS errors less than 0.25 m for significant wave height and 1.7 m s⁻¹ for 10 m wind speed.

SES BEHAVIORAL VARIABLES

During post-dive surfacing time, SES rise to the ocean surface in order to breathe, remaining continuously close to vertical with only their heads out of the water (Génin et al., 2015). This behavior has been modeled with the Euler angles pitch, roll, and yaw (the yaw variable is also referred to as heading in the literature).

It is computed from raw magnetometer data $M = (m_x, m_y, m_z)$ and accelerometer data $A = (a_x, a_y, a_z)$ that are classically used to characterize aircraft principal axes (Rajeswari and Suresh, 2015). Following the standard convention from aeronautics, we assume that a frame attached to the body is set such that x is pointing forward, z up, and y is to the animal's left. Then, the body rotation is defined by first applying a rotation around z (yaw), then a rotation around the resulting y (pitch), and finally a rotation around the resulting x (roll) (Rajeswari and Suresh, 2015). Put into equations, after normalization of accelerometer data $A = A / \|A\|$, which assumes that the system mostly measures the acceleration due to gravity, we have

$$\text{Pitch} = -\arcsin(a_x)$$

$$\text{Roll} = \arcsin\left(\frac{a_x}{\cos(\text{Pitch})}\right).$$

When the tag is not aligned perfectly, the compass data must be integrated with the accelerometer data; sometimes called “tilt compensation,” this is a standard feature of hand-held compasses (Rajeswari

and Suresh, 2015). The Acousonde 3A does not offer built-in tilt compensation, but knowing the roll and pitch angle, the following operator is used to rotate the magnetometer and acceleration variables back to the horizontal plane:

$$O^h = \begin{pmatrix} \cos(-\text{Pitch}) & 0 & \sin(-\text{Pitch}) \\ 0 & 1 & 0 \\ -\sin(-\text{Pitch}) & 0 & \cos(-\text{Pitch}) \end{pmatrix} \cdot \begin{pmatrix} 1 & 0 & 0 \\ 0 & \cos(-\text{Roll}) & -\sin(-\text{Roll}) \\ 0 & \sin(-\text{Roll}) & \cos(-\text{Roll}) \end{pmatrix}$$

These rotated magnetometer and acceleration data are written as $M^h = O^h \cdot M = (m_x^h, m_y^h, m_z^h)$ and $A^h = O^h \cdot A = (a_x^h, a_y^h, a_z^h)$, respectively, where a_z^h is the vertical acceleration projected horizontally. M^h is used to compute the yaw variable as follows:

$$\text{Yaw} = \text{atan2}(m_y^h, m_x^h)$$

Figure 3 presents a cartoon of the environmental and behavioral variables and how they relate to each other. For example, in the absolute coordinate system (in purple), the variables yaw and z^h (vertical

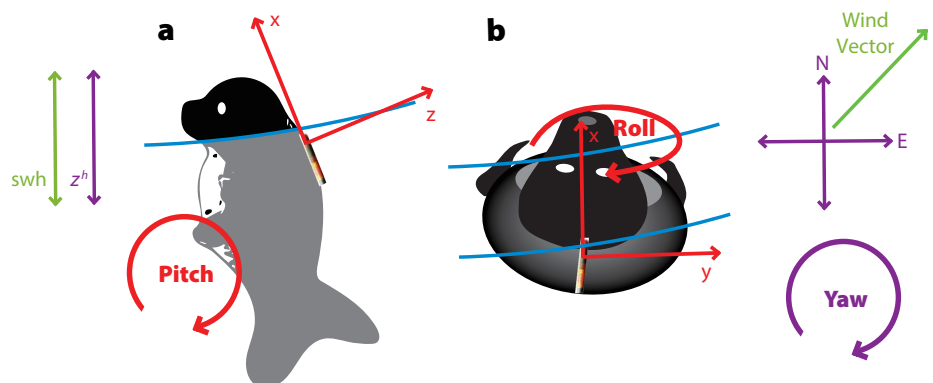


FIGURE 3. Cartoon explanation of environmental and SES behavioral variables with (a) side and (b) top views. Red plots indicate variables and coordinate systems relative to the SES frame, and purple those that are relative to the absolute coordinate system.

¹ For any real number (e.g., floating point) arguments x and y not both equal to zero, $\text{atan2}(y, x)$ is the angle in radians between the positive x -axis of a plane and the point given by the coordinates (x, y) .

displacement projected horizontally) can be directly compared to wind direction and significant wave height (swh). Variables pitch, roll, and yaw used in the following analysis are composed of successive post-dive surface intervals concatenated over time.

Methods for Hypothesis (1)

To test our first hypothesis, that SES behavior is constrained by wind speed and/or direction, pair-wise scattering plots and Pearson correlation coefficients were computed between all possible pairs of SES (i.e., pitch, roll, yaw) and environmental variables (i.e., ψ_W , φ_W , swh). Prior to analysis, all of these variables were median averaged every 10 s and standardized (i.e., zero mean and unitary variance). Linear regression fitting models were then applied to each variable pair using environmental variables to explain SES behavioral variables. Outliers to these models were identified as the model values with a Cook's distance exceeding three times the mean of this distance.

Then, after removal of these outliers, a second linear regression model is applied to the data, and the Pearson correlation coefficient P and the p-value statistical hypothesis testing were computed.

Methods for Hypothesis (2)

To test our second hypothesis, that SES can be used as weather buoys to estimate wave parameters, we followed classical methods of wave statistics applied to weather buoy sensor data (e.g., Earle, 1996). We first computed the one-sided power spectral density (PSD) of the raw accelerometer data a_z^h . PSDs were then high-pass filtered with a frequency cutoff at 20 s in order to reduce the low-frequency “noise” effects that are out of the expected wave band. The choice of this cutoff frequency was justified as follows. After scanning the mean wave period (from the variable mwp, ECMWF ERA-Interim) of the Southern Ocean from October to December 2011 and 2012, we observed that the waves in our recording area were not expected to have

periods longer than 20 seconds² (as is the case for most oceanic waves). As a result, this cutoff frequency for high-pass filtering reduced the low-frequency noise problem without removing wave information for statistical estimates of dominant wave period. Note that such a cutoff frequency has already been used in literature (e.g., Irish et al., 2002; Lin et al., 2017). Then, wave spectra (also called displacement spectra) were obtained by dividing acceleration PSDs by the angular frequency to the fourth power (Hashimoto and Konbune, 1988). Zero-crossing periods were eventually calculated from wave spectra based on the method given by Earle (1996, p. 12). This wave period, commonly called mean wave period, is defined by the whole ensemble of wave components.

To help interpret our results, we designed a simple factor Q that quantifies the degree of monochromaticity of wave spectra. A spectrum is monochromatic when it exhibits one salient spectral peak over its frequency range. Also, multiple peaks in our wave spectra come from SES behavior and/or multiple ocean wave components, and we will not try within this study to reconcile the ambiguities between these two contributions. This Q factor is defined as

$$Q = \text{findpeaks}(N_p, \text{SNR}),$$

where Q is computed using the built-in MATLAB function *findpeaks*, with custom parameters N_p that measure the number of spectrum peaks above a certain threshold, and SNR that measures the salience of each peak.

RESULTS

Analysis of Hypothesis (1)

Regarding the first hypothesis, Figure 4 shows the first four most-correlated variables for the SES individual associated with Acousonde A031: (a) yaw/ ψ_W , (b) roll/ ψ_W , (c) pitch/ φ_W , and (d) pitch/swh. No significant rela-

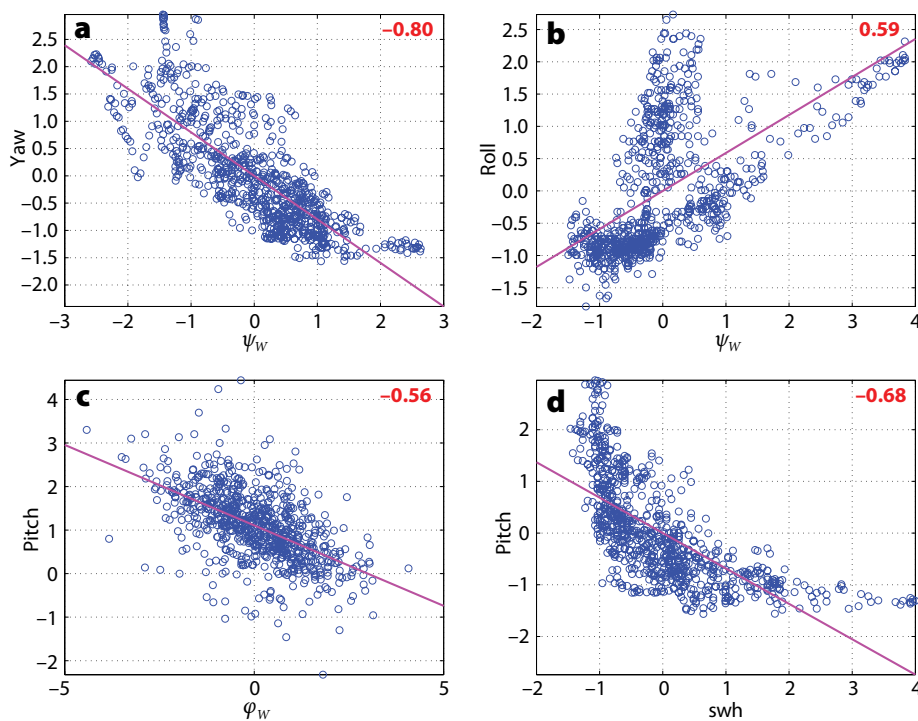


FIGURE 4. Pair-wise scattering plots and Pearson correlation coefficients (in red) resulting from robust linear fitting models between the following variable pairs: (a) yaw/ ψ_W , (b) roll/ ψ_W , (c) pitch/ φ_W , and (d) pitch/swh, for the SES individual equipped with Acousonde A031 instruments. Note that the x-axes are not similar in the different columns due to outlier removals in the robust linear fitting models. All these variables are standardized (i.e., zero mean and unitary variance).

² Actually, the mwp variable provided by ECMWF did not exceed 17 s.

tionships emerged from other variable pairs. Wind direction ψ_W is an efficient explanatory variable for the SES yaw, with $P = -0.80$ (p-value < 0.001), and to a lesser extent, for the SES pitch variable, with $P = -0.59$ (p-value < 0.005). The wind speed norm φ_W was an efficient explanatory variable for SES pitch, with $P = -0.56$ (p-value < 0.001). Significant wave height swh was an efficient explanatory variable for SES pitch, with $P = -0.68$ (p-value $= 0.003$). In fact, all analyzed environmental variables have a strong correlation (i.e., $|P| > 0.55$, p-value < 0.001), with at least one behavioral response of the SES. Furthermore, we note that in regression models, outliers should follow a normal distribution with matched variance for the model to be valid. This condition is well respected across our different models.

We also performed an in-depth analysis of the outliers (see section Methods for Hypothesis (1) for their definition) resulting from these linear regression models. Table 3 characterizes the outliers resulting from the two regression models $\text{yaw} \sim \psi_W$ and $\text{pitch} \sim \varphi_W$, where ψ_W and φ_W are the explanatory (i.e., environmental) variables of these models, respectively. In particular, we were interested in the value intervals of the different environmental variables where these outliers mainly fall. In the Table 3 columns below “Environmental Variables,” their 90th percentile intervals are displayed. When compared to the full environmental range of values, we note that it is globally the low values of wind speed that tend to reject the linear regression fitting models. As an illustrative example, the 90th percentile of outliers from the model $\text{yaw} \sim \psi_W$ is composed of φ_W values inferior to 8 m s^{-1} (in regards to its full range of $[2; 28] \text{ m s}^{-1}$). For the model $\text{pitch} \sim \varphi_W$, this interval is slightly larger, $[2; 13] \text{ m s}^{-1}$. A similar comment can be made for the values of outliers within the variable swh, which also has low values. On the contrary, the range intervals of these outliers within the ψ_W variable almost overlap with the full range of

values (i.e., $[-2.8; 2.9] \text{ rad}$, see Table 2).

Figure 5 provides correlation diagrams, where each pair-wise Pearson correlation coefficient is displayed in each cell and shaded according to its value (from white to dark, 0 to 1). The different panels a–d correspond to the four different SES individuals equipped with Acousondes. Among these diagrams, the previously highlighted pair-wise correlation relations are well preserved, with inter-individual variations in p-values that on average remain below 0.2.

Analysis of Hypothesis (2)

Regarding the second hypothesis, Figure 6 provides two examples of the variable a_z^h during two post-dive surface intervals of the SES individual equipped

with Acousonde A626019. The upper panels are raw time series plots. At the bottom, power spectral densities of vertical displacements, computed from the acceleration time series, are plotted against a wave period (in s) vector ranging from 2 s to 20 s. We superimposed in red to this spectrum the reference values for mean wave period. Example (a) exhibits a high monochromaticity factor Q of 0.95, with the presence of a clear and salient wave period peak that fits very well the mean wave period value. In contrast, a monochromaticity factor Q of 0.13 has been computed for example (b), as its spectrum exhibits multiple peaks and a non-monochromatic content.

Figure 7 provides a large-scale result over all post-dive surface intervals for the

TABLE 3. Analysis of the outliers resulting from the linear regression models displayed in Figure 4. The left column shows the different regression models, formatted as $\text{yaw} \sim \psi_W$ and $\text{pitch} \sim \varphi_W$, where ψ_W and φ_W represent the response (i.e., behavioral) and explanatory (i.e., environmental) variables, respectively. The 90th interval values of their outliers are shown within the different environmental variables.

Regression Model	Percentage of Outliers	Environmental Variables		
		ψ_W	φ_W	swh
Yaw $\sim \psi_W$	11	$[-2.1; 2.2]$	$[2; 8]$	$[1; 5]$
Pitch $\sim \varphi_W$	16	$[-2.4; 2.8]$	$[2; 13]$	$[1; 6]$

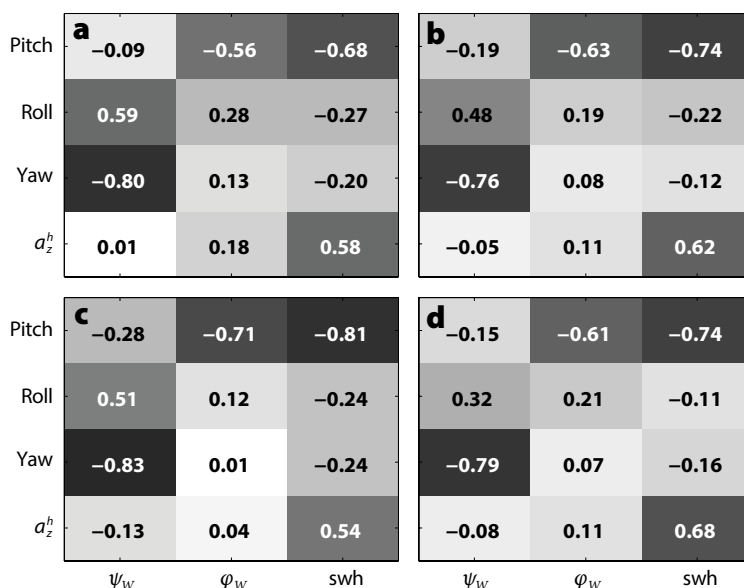


FIGURE 5. Correlation diagrams for the four SES individuals equipped with Acousondes: (a) A031, (b) A032, (c) 626019, and (d) 626040. Each pair-wise Pearson correlation coefficient is displayed in each cell and shaded according its absolute value (from white to dark, 0 to 1).

SES individual equipped with Acousonde 626019. On graph (a), we superimposed all estimates (in blue) with the reference values provided by the variable mwp (in red). On graph (b), the monochromaticity factor Q associated with each estimate is plotted. Globally, it shows high variability. Interestingly, around the dates of November 3, 2012, to November 6, 2012, and November 17, 2012, to November 20, 2012, slight increases in the value offset are seen. On graph (c), we superimposed mwp values and the mean wave period estimations with a Q higher to their 90th percentile. We observe that estimates associated with a high Q value fit the mwp values well through the entire duration of data recording, especially during the two time periods mentioned above.

Interestingly, these time periods also correspond to higher mwp values, which themselves correspond to higher values of swh (a Pearson correlation of $P = 0.91$, p -value < 0.001 , has been computed between the two variables).

Figure 8 provides histograms of the error ε_{mwp} , computed as the absolute difference between the estimation and the reference values of mean wave period. The different histograms a to d correspond to the four different SES individuals. Filtering of mwp estimates through the Q factor (i.e., the Q -filtered estimations) allowed us to maintain estimation errors below 2 s, except for a few marginal estimations. The different SES individuals show great consistency, exhibiting very similar error distribution patterns.

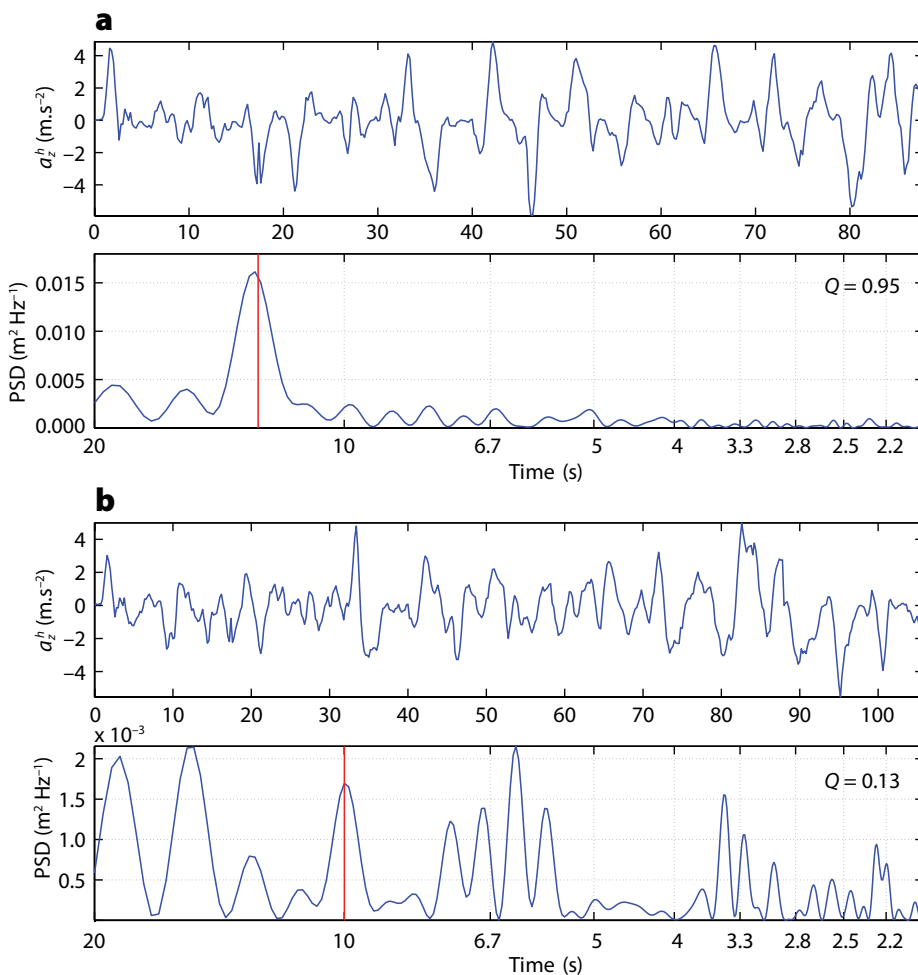


FIGURE 6. Two examples of a_z^h (upper panels in a and b) and power spectral densities (PSD) of their vertical displacements (lower panels). The vertical red lines in the spectral densities correspond to the mean wave period (mwp), considered as the reference value for this parameter. These graphs also display the monochromaticity factors Q . Example (a) corresponds to a highly monochromatic wave spectrum (with $Q = 0.95$), and (b) to a low one (with $Q = 0.13$).

DISCUSSION

There are two main limitations to this study. First, because we did not use a reference magnetic field for Kerguelen Island to define magnetic north, we assume the magnetic field to be locally constant. The consequence of this uncertainty is that there is a constant offset between the measured compass angle and true magnetic north; however, we are still able to correlate wind headings and the animals' preferred orientations, taking into account this offset. Precise magnetic field referencing would be required to define the value of the preferred SES alignment with respect to the wind. Furthermore, both accelerometer and magnetometer data lack in situ calibration with local environmental parameters and SES behavior. Taken altogether, these material limitations restrict our analysis to relative variations. Second, measurements with satellite imaging are not exempt from errors, and error checking procedures are not reliable either, as no ground truth data exist to validate them, especially in open ocean areas (Berrisford et al., 2011).

Regardless, this study clearly reveals that sea state and above-surface meteorological conditions constrain some long-term trends in SES surface behavior. Studying such trends can potentially provide scientists with valuable information about the ocean environment. Linear fitting models and a Pearson correlation analysis were performed to investigate the relationship between SES behavior at the surface (i.e., pitch, roll, yaw) and above-surface environmental conditions (i.e., ψ_W : wind direction, φ_W : wind speed norm and significant wave height). Our analysis reveals that for four different SES individuals recorded in two successive years, there are strong consistent correlations between certain pairs of variables. In particular, wind direction ψ_W was sufficiently predicted by the SES yaw and roll, and wind speed norm φ_W by the SES a_z^h and pitch. Significant wave height was an efficient explanatory variable for the SES a_z^h and pitch. Outliers to these linear regression models correspond

globally to low values of explanatory variables (e.g., 90th percentile of the outliers from the linear regression $yaw \sim \psi_W$ have wind speed norm values below 8 m s^{-1}). In other words, SES behavior at the surface is less constrained by the environment for low values of wind speed. We interpret this result as an indication that under high wind conditions, SES mostly orient their heads at the surface, along with their bodies, to avoid ocean spray by facing away from the wind and wind-generated waves, which could inhibit breathing. This behavior tends to disappear with decreasing wind strength, with the SES exhibiting more erratic orientation. It should be added that these tendencies seem to be preserved from one individual to another (Figure 5). It is also noteworthy that the pitch variable appears to correlate well with both wind speed and significant wave height, providing a possible insight into the known relation between local wind speed and significant wave height (Lin et al., 2017). We acknowledge that the correlation analysis could have been optimized using more complex methods (e.g., nonlinear regression), but our goal in this study was mainly to illustrate that a basic analysis (i.e., a linear regression) is enough to extract useful information within our experiments.

Mean wave period was estimated based on wave spectra computed from SES vertical acceleration during SES time at the surface. We paid special attention to monochromatic wave spectra (i.e., with only one salient spectral peak), which were filtered using a Q factor (see computation details in the section on Methods for Hypothesis [2]). Keeping only estimates with a Q higher than the 90th percentile of Q, our results on mean wave period exhibit errors below 2 s. In short, when an SES exhibits a strong vertical periodic oscillation, that time period corresponds well to the period of a single ocean swell. This would suggest that SES drift along ocean swells, most likely to maximize their comfort, stability, and energy recovery while at the surface. We also observed that the surface-following

behavior of SES gets stronger with higher wave periods, and also with higher wave heights. Consequently, our estimates of mean wave period seem to improve for higher wave height values. Also, as

discussed above, these estimates are well preserved from one individual to another (Figure 8). This unified SES behavior in response to environmental parameters supports the possibility that they could

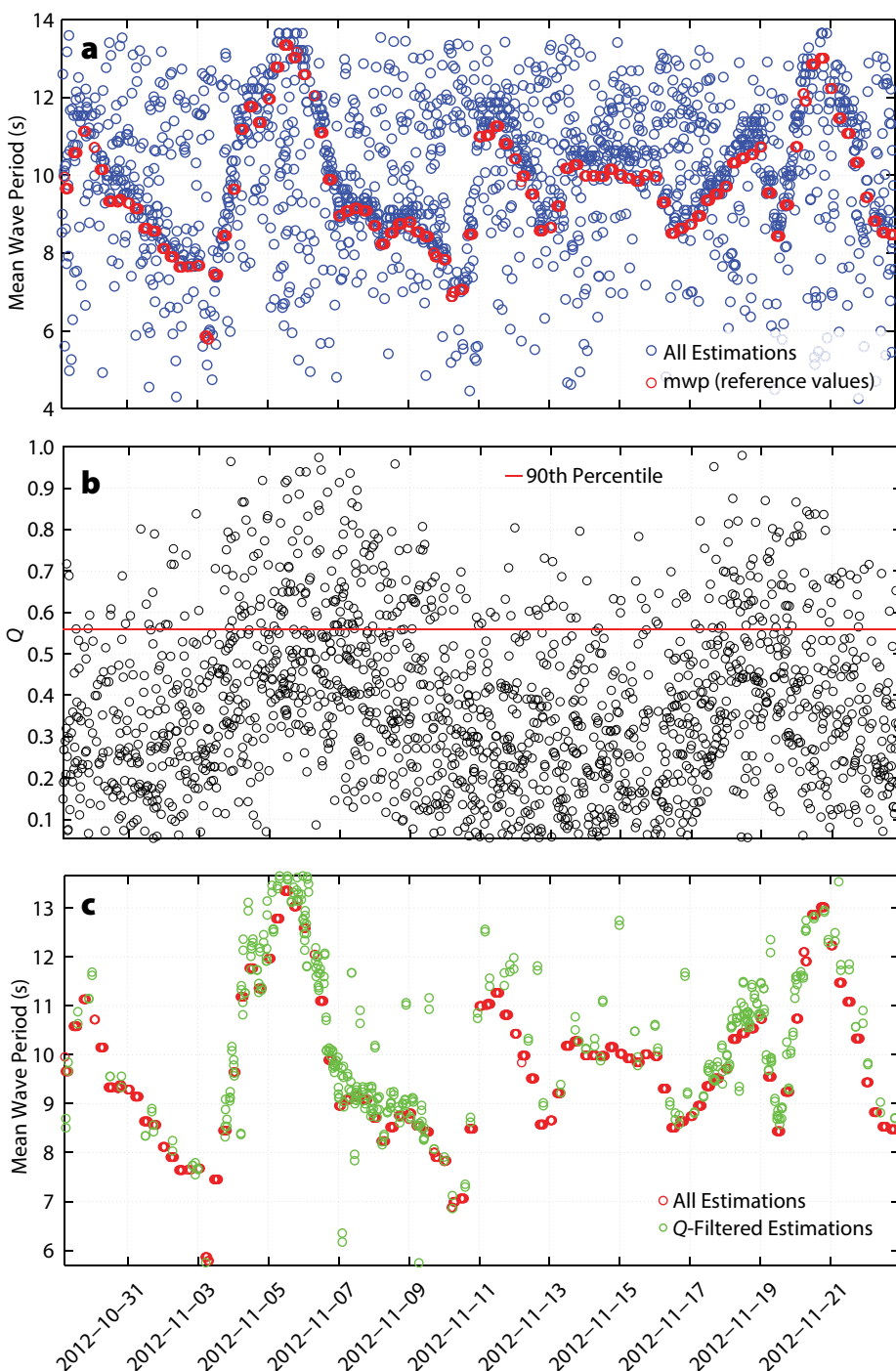


FIGURE 7. Estimate of the mean wave period, following procedure detailed in the text section on Methods for Hypothesis (2). In (a), all estimates (in blue) and reference values (i.e., mwp, in red) of mean wave period are computed for all phase surfaces of the SES individual equipped with Acousonde 626019. In (b), Q (monochromaticity factor) values of each estimate are superimposed on the 90th percentile of this factor (red line). In (c), estimation values of mean wave period with a Q higher than the 90th percentile of this factor (in green circles) are shown with reference values (i.e., mwp, in red) of mean wave period.

be used as proxies to measure wind direction and wave period. When considering the full set of wave spectra, independent from the monochromaticity factor values, our estimated mean wave periods span a larger error range (up to 9 s), which corresponds to non-monochromatic signals that may result from more complex SES behavior and/or ocean wave patterns. We also tested a higher cutoff frequency for the high-pass filter for the mean wave period estimation, passing from 20 to 30 s. In doing so, we take into account a lower frequency part of the sea swell band. We observed that this modification only marginally affected the Q-filtered estimations.

To put in perspective the obtained average error of mean wave period, we note that Anttil et al. (1993) and Earle and Borgman (1999) compared National Data Buoy Center wave heights and periods with those obtained from a wave staff and a biaxial current meter fixed to nearby Bullwinkle platforms. Ninety-five percent of significant wave heights agree within 0.2 m, and 95% of dominant wave periods agree within 0.7 s. These excellent results would not have been possible without the use of a sea-state-dependent variable for noise corrections. In our estimates of wave parameters, we did not apply such a noise correction filter, nor


did we use optimization operations to better fit our estimates to the ground-truth values. In addition, our error estimation procedure cannot be as accurate as that computed for weather buoys (in particular, due to the intrinsic error of satellite imaging). Despite these experimental limitations, our preliminary results are satisfying and promising for future research in this direction.

CONCLUSION

In this study, we used accelerometer and magnetometer data from biologged southern elephant seals to evaluate whether ocean environmental parameters influence their behavior during post-dive surfacing time. Our results showed that long-term trends of SES behavior at the surface, modeled with Euler angles characterizing its three-dimensional dynamics, are constrained by wind direction, significant wave height, and mean wave period.

This study demonstrates that biologged SES can provide valuable field-based auxiliary data for monitoring the global ocean environment. The high-resolution temporal sampling acquired with biologged SES complements large-scale satellite imaging. We demonstrated that biologged SES could be used as oceanographic samplers to estimate wind direction and

wave period. The biologging technology (including Acousonde 3A) used on the SES also offers a multimodal acquisition capability, transforming SES into integrative measurement platforms capable of collecting important in situ environmental information. For example, current estimations on mean wave parameters could be combined with acoustic-based wind speed estimation (Cazau et al., 2017).

Despite the accomplishments of our study, many questions remain open regarding the more general aspects of the relationship between SES biology and environmental forcing. Additional research is needed to explore these questions. 

REFERENCES

- Anttil, F., M.A. Donelan, G.Z. Foristall, K.E. Steele, and Y. Ouelle. 1993. Deep water field evaluation of the NDBC-SWADE 3-m discus directional buoy. *Journal of Atmospheric and Oceanic Technology* 10:97–112.
- Bailleul, F., M. Authier, S. Ducatez, F. Roquet, J.B. Charrassin, Y. Cherel, and C. Guinet. 2010. Looking at the unseen: Combining animal biologging and stable isotopes to reveal a shift in the ecological niche of a deep-diving predator. *Ecography* 33:709–719, <https://doi.org/10.1111/j.1600-0587.2009.06034.x>.
- Berrisford, P., D.P. Dee, P. Poli, R. Brugge, K. Fielding, M. Fuentes, P.W. Källberg, S. Kobayashi, S. Uppala, and A. Simmons. 2011. *The ERA-Interim Archive Version 2.0*. ERA Report Series, European Centre for Medium Range Weather Forecasts, Reading, UK, 23 pp.
- Burgess, W.C. 2000. The bioacoustic probe: A general-purpose acoustic recording tag. *Journal of the Acoustical Society of America* 108(5):2,583–2,583, <https://doi.org/10.1121/1.4743598>.
- Burgess, W.C., P. Tyack, B. Le Boeuf, and D.P. Costa. 1998. A programmable acoustic recording tag and first results from free-ranging northern elephant seals. *Deep Sea Research Part II* 45:1,327–1,351, [https://doi.org/10.1016/S0967-0645\(98\)00032-0](https://doi.org/10.1016/S0967-0645(98)00032-0).
- Cazau, D., J. Bonnel, J. Joumaa, Y. Le Bras, and C. Guinet. 2017. Measuring the marine soundscape of the Indian Ocean with southern elephant seals used as acoustic gliders of opportunity. *Journal of Atmospheric and Oceanic Technology* 34:207–223, <https://doi.org/10.1175/JTECH-D-16-0124.1>.
- Charrassin, J.B., M. Hindell, S.R. Rintoul, F. Roquet, S. Sokolov, M. Biuw, D. Costa, L. Boehme, P. Lovell, R. Coleman, and others. 2008. Southern Ocean frontal structure and sea-ice formation rates revealed by elephant seals. *Proceedings of the National Academy of Sciences of the United States of America* 105:11, 634–11, 639, <https://doi.org/10.1073/pnas.0800790105>.
- Daniault, N.P., P. Blouch, and F.X. Fusey. 1985. The use of free-drifting meteorological buoys to study winds and surface currents. *Deep Sea Research Part A* 32(1):107–113, [https://doi.org/10.1016/0198-0149\(85\)90020-2](https://doi.org/10.1016/0198-0149(85)90020-2).
- Day, L., J. Joumaa, J. Bonnel, and C. Guinet. 2017. Acoustic measurements of post-dive cardiac responses in southern elephant seals

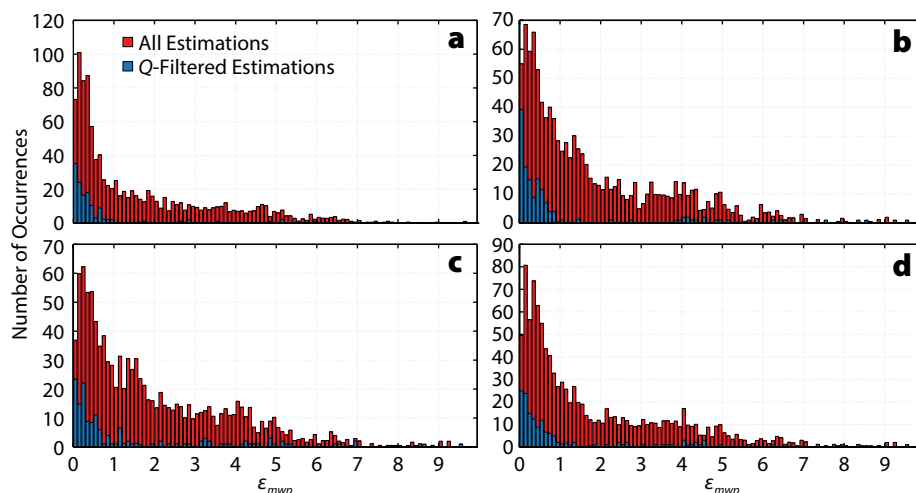


FIGURE 8. Histograms of the errors ϵ_{mwp} in the estimation of mean wave period for the four different Acousondes: (a) A031, (b) A032, (c) 626019, and (d) 626040. Red bars represent errors obtained with the complete set of estimations, while blue bars represent errors obtained with estimations having a Q factor higher than the 90th percentile of this factor.

- (*Mirounga leonina*) during surfacing at sea. *Journal of Experimental Biology* 220:1,626–1,633, <https://doi.org/10.1242/jeb.146928>.
- Dee, D.P., S.M. Uppala, and A.J. Simmons. 2011. The ERA-Interim Reanalysis: Configuration and performance of the data assimilation system. *Quarterly Journal of the Royal Meteorological Society* 137:553–597, <https://doi.org/10.1002/qj.828>.
- Earle, M.D. 1996. *Nondirectional and Directional Wave Data Analysis Procedures*. National Data Buoy Center Technical Document 96-01. National Oceanic and Atmospheric Administration, US Department of Commerce, Stennis Space Center, MS, USA, 43 pp., <http://www.ndbc.noaa.gov/wavemeas.pdf>.
- Earle, M.D., and L.E. Borgman. 1999. Statistical inter-comparison of ocean wave parameters. Paper presented at the Third Conference on Coastal Atmospheric and Oceanic Prediction and Processes, November 3–5, 1999, New Orleans, LA, American Meteorological Society.
- Génin, A., G. Richard, J. Jouma'a, B. Picard, N. El Ksabi, J. Vacquie-Garcia, and C. Guinet. 2015. Characterization of postdive recovery using sound recordings and its relationship to dive duration, exertion, and foraging effort of southern elephant seals (*Mirounga leonina*). *Marine Mammal Science* 31:1,452–1,470, <https://doi.org/10.1111/mms.12235>.
- Gilhouse, D.B. 2007. Improvements in National Data Buoy Center measurements. National Oceanic and Atmospheric Administration, <http://www.ndbc.noaa.gov/improvements.shtml>.
- Guinet, C., J. Vacquie-Garcia, B. Picard, G. Bessigneul, Y. Le Bras, A.C. Dragon, M. Viviant, J.P.Y. Arnould, and F. Bailleul. 2014. Southern elephant seal foraging success in relation to temperature and light conditions: Insight into prey distribution. *Marine Ecology Progress Series* 499:285–301, <https://doi.org/10.3354/meps10660>.
- Guinet, C., X. Xing, E. Walker, P. Monestiez, S. Marchand, B. Picard, T. Jaud, M. Authier, C. Cotté, A.C. Dragon, and others. 2013. Calibration procedures and first dataset of Southern Ocean chlorophyll profiles collected by elephant seals equipped with a newly developed ctd-fluorescence tags. *Earth Systems Science Data* 5:15–29, <https://doi.org/10.5194/essd-5-15-2013>.
- Hashimoto, N., and K. Konbune. 1988. Directional spectrum estimation from a Bayesian approach. *Coastal Engineering Proceedings* 1:62–7.
- Hindell, M.A. 1991. Some life-history parameters of a declining population of southern elephant seals, *Mirounga leonina*. *Journal of Animal Ecology* 60:119–134.
- Irish, J.D., D.W. Fredriksson, and J. Ahern. 2002. *Estimating Significant Wave Height and Dominate Wave Period from Buoy Mounted, Strap-Down Accelerometer Observations*. Technical report, Woods Hole Oceanographic Institution, 24 pp.
- Lin, Y.-P., C.-J. Huang, S.-H. Chen, D.-J. Doong, and C.C. Kao. 2017. Development of a GNSS buoy for monitoring water surface elevations in estuaries and coastal areas. *Sensors* 17(1):172, <https://doi.org/10.3390/s17010172>.
- Rajeswari, V., and L.P. Suresh. 2015. Investigation and control of principal axes of aircraft using robust method. In *Power Electronics and Renewable Energy Systems*. C. Kamalakannan, L. Suresh, S. Dash, and B. Panigrahi, eds, Lecture Notes in Electrical Engineering, vol. 326, Springer, New Delhi, https://doi.org/10.1007/978-81-322-2119-7_152.
- Richard, G., J. Vacquie-Garcia, J. Jouma'a, B. Picard, A. Génin, J.P.Y. Arnould, F. Bailleul, and C. Guinet. 2014. Variation in body condition during the post-moult foraging trip of southern elephant seals and its consequences on diving behaviour. *Journal of Experimental Biology* 217:2,609–2,619, <https://doi.org/10.1242/jeb.088542>.
- Ropert-Coudert, Y., and R.P. Wilson. 2005. Trends and perspectives in animal-attached remote sensing. *Frontiers in Ecology and the Environment* 3:437–444, [https://doi.org/10.1890/1540-9295\(2005\)003\[0437:TAPIAR\]2.0.CO;2](https://doi.org/10.1890/1540-9295(2005)003[0437:TAPIAR]2.0.CO;2).
- Roquet, F., G. Williams, M.A. Hindell, R. Harcourt, C. McMahon, C. Guinet, J.-B. Charrassin, G. Riverdin, L. Boehme, P. Lovell, and M. Fedak. 2014. A southern Indian Ocean database of hydrographic profiles obtained with instrumented elephant seals. *Scientific Data* 1:140028, <https://doi.org/10.1038/sdata.2014.28>.
- Rutz, C., and G.C. Hays. 2009. New frontiers in biologging science. *Biology Letters* 5:289–292, <https://doi.org/10.1098/rsbl.2009.0089>.
- Stopa, J.E., and K.F. Cheung. 2014. Intercomparison of wind and wave data from the ECMWF Reanalysis Interim and the NCEP Climate Forecast System Reanalysis. *Ocean Modelling* 75:65–83, <https://doi.org/10.1016/j.ocemod.2013.12.006>.
- Treasure, A.M., F. Roquet, I.J. Ansorge, M.N. Bester, L. Boehme, H. Bornemann, J.-B. Charrassin, D. Chevallier, D.P. Costa, M.A. Fedak, and others. 2017. Marine Mammals Exploring the Oceans Pole to Pole: A review of the MEOP consortium. *Oceanography* 30(2):132–138, <https://doi.org/10.5670/oceanog.2017.234>.
- Williams, G.D., L. Herraiz-Borreguero, F. Roquet, T. Tamura, K.I. Ohshima, Y. Fukamaic, A.D. Fraser, L. Gao, H. Chen, C.R. McMahon, and others. 2016. The suppression of Antarctic Bottom Water formation by melting ice shelves in Prydz Bay. *Nature Communications* 7:12577, <https://doi.org/10.1038/ncomms12577>.

ACKNOWLEDGMENTS

This study is part of a national research program (no. 109, H. Weimerskirch and the observatory Mammifères Explorateurs du Milieu Océanique, MEMO SOERE CTD 02) supported by the French Polar Institute (Institut Paul Emile Victor, IPEV). This work was carried out in the framework of the ANR Blanc MYCTO-3D-MAP and ANR VMC 07: IPSOS-SEAL programs and CNES-TOSCA program “Éléphants de mer océanographes.” The authors also thank the Total Foundation for financial support. All animals in this study were treated in accordance with the IPEV ethical and Polar Environment Committees guidelines. We thank all the people who contributed to the fieldwork and data processing, with special acknowledgments to M. Authier, A. Chaigne, Q. Delorme, N. El Skaby, J.C. Vaillant, and F. Vivier. We are extremely grateful to the two anonymous referees and the two editors for their constructive suggestions and the detailed corrections provided. The authors also would like to kindly thank Dimitri Sourzac for his help with the drawing of Figure 3.

AUTHORS

Dorian Cazau (cazaudorian@outlook.fr) is Postdoctoral Researcher, ENSTA Bretagne, Lab-STICC (UMR CNRS 6285), Brest, France. **Cédric Pradalier** is Assistant Professor, GeorgiaTech Lorraine - UMI 2958 GT-CNRS, 2, Metz, France. **Julien Bonnel** is Assistant Professor, ENSTA Bretagne, Lab-STICC (UMR CNRS 6285), Brest, France. **Christophe Guinet** is CNRS Research Scientist, Centre d'Etudes Biologiques de Chizé, UMR 7372 Université de La Rochelle-CNRS, Villiers en Bois, France.

ARTICLE CITATION

Cazau, D., C. Pradalier, J. Bonnel, and C. Guinet. 2017. Do southern elephant seals behave like weather buoys? *Oceanography* 30(2):140–149, <https://doi.org/10.5670/oceanog.2017.236>.